

Simulation and Validation of Random-Modulation Continuous Wave on LED Mini-Lidar

Prane Mariel ONG^{1,2}, Hiroaki KUZE^{1,2}, and Tatsuo SHIINA¹

¹Chiba University, 1-33 Yayoi-cho, Inage-ku, Chiba, 263-8522

²Center for Environmental Remote Sensing (CEReS), Chiba University, 1-33 Yayoi-cho, Inage-ku, Chiba 263-8522

Abstract: A compact LED lidar was constructed and field-tested with the aim to observe the Mars' dust devils. It was constructed to fit a 10 cm-cube dimension limit. In its present form, it has a 0.75W (7.5nJ/10ns) pulse power, and 500 kHz pulse repetition frequency. These parameters were optimized to observe fast-moving targets (i.e. dust, smoke, etc.) in the near range. Although, it is limited to nighttime measurement, the result from the signal-to-noise ratio (SNR) simulations show that the pseudo random modulated continuous wave (RM-CW) technique was able to increase its SNR by about 4 orders of magnitude given one second iteration and considering the skylight condition.

Key Words: LED lidar, RM-CW, SNRs

1. Introduction

An LED mini lidar system was designed and constructed to meet the size restrictions of a Mars rover and to quantitatively measure the dust devils on Mars surface¹. Dust devils comprises of rotating columns of air that pick-up dust and debris from the ground surface. Thus, in situ measurements of near-ground atmospheric and dust activities on Mars will be useful in the study of this phenomenon.

To date several experiments have been conducted to assess the LED mini lidar's performance and assimilate fast-moving targets (i.e. smoke, mist, sea wave, near-ground dust, and twister²). Initially, we conducted experiments in a controlled environment. Such environment is the wind tunnel in Japan Meteorological Agency (JMA) to monitor the smoke's flow, diffusion and convection. The wind speed and direction were controlled so system corrections and calibrations can be made. Then, we utilized the twister generator in Nagoya Science Museum to derive the spatial distribution of a twister's cross-section. Despite all of these, the current pulse LED mini lidar is still limited to nighttime observation or when the background light intensity is not too high.

To be able to improve the current LED mini lidar's performance, we need to increase its signal-to-noise ratio (SNR). Referring to the derived SNR equation of a pulse lidar by Takeuchi, et al.,³ it is expressed as,

$$\left(\frac{S}{N}\right)_{\text{pulse}} = \frac{\sqrt{M}\sqrt{\xi}P_p g(t)\Delta t}{\sqrt{P_p g(t)\Delta t + 2b}} \quad (1)$$

where M is the accumulated number of pulses over a given time, ξ is the conversion constant from power to photoelectron number ($\xi = \Delta t \eta_Q / h\nu$, Δt : pulse temporal width, η_Q : detector's quantum efficiency, h : Planck's constant, ν : frequency), P_p is the light's peak power, $g(t)$ lidar response function, and b is the background noise. Derived from the lidar's equation, the response function is given by this equation,

$$g(t) = \frac{c}{2} AK \frac{Y(R)}{R^2} \beta(R) T(R)^2 \quad (2)$$

where c is the speed of light, A is the telescope's receiving area, K is the telescope's receiving efficiency, $Y(R)$ is the overlap function, R is the distance to the target, $\beta(R)$ is the backscattering coefficient at the position of the target at distance R , and $T(R)$ is the light transmittance through the atmosphere. $b = AK S_b \frac{\pi}{4} \theta_{FOV}^2$, where θ_{FOV} is the receiver's field of view, and S_b the is solar radiance $\sim 0.08 \text{ Wm}^{-2}\text{sr}^{-1}\text{nm}^{-1}$.

From Eq. 1, there are a few ways to improve the SNR of the LED lidar. Increasing the accumulated number of pulses, increasing the receiver's effective area, and increasing the output power of the transmitter are just a few examples. Increasing M , is the usual choice. However, it will hinder measuring fast



Fig. 1. LED mini lidar in biaxial configuration with angle adjuster configured for near-range ground observation.

moving targets. Since the LED lidar system is size constraint, increasing the receiver's effective area is not an ideal option. In order to improve the output power of the current LED lidar system, we will utilize the RM-CW technique (random modulated continuous wave), which was first introduced by Takeuchi, et al.³⁻⁵⁾

In this paper, we present a simulation result of the SNR comparison between a pulse LED lidar and RM-CW LED lidar. In addition, we also included the SNR simulation result for 1W LD as a reference lidar.

2. Pulse vs RM-CW

RM-CW lidar transmits a continuous pseudo-randomly modulated pulses into the atmosphere in a similar manner as a pulse lidar does. The only difference is the number of pulses in one period iteration (one code cycle). The most common modulation code is the M sequence, which is generated by a linear shift register. Figure 2 shows a synced pulse modulated signal and an M sequence signal. M sequence is a type of pseudorandom binary sequence (PRBS).

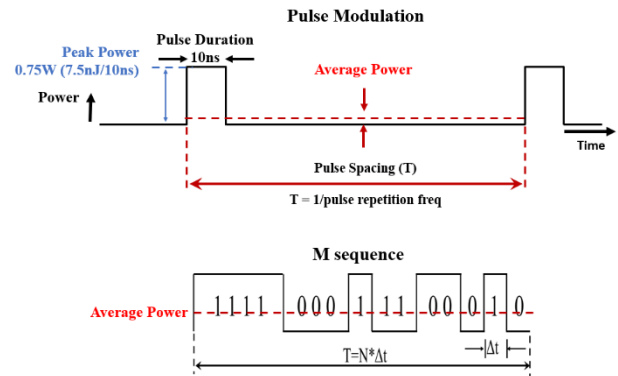


Fig. 2. Comparison of an M sequence of length 15 bits ($N = 15$) synced to a pulse modulation with respect to one period iteration.

3. M-sequence

M-sequence is a binary series given N total number of elements, a_i . Mathematically, the elements of an M-sequence should be represented by an absolute value of 1. If we convert the set a_i : (1,0) to a'_i : (1,-1) then we get this relation $a'_i = 2a_i - 1$. And due to the δ -function-like autocorrelation property of M sequence, it permits the signal demodulation by correlation.

The cross correlation of a'_i to a_i is given by

$$\phi_{aa'} = \sum_{i=0}^{N-1} a_i a'_{i+j} = \begin{cases} \frac{N+1}{2} & j = 0 \pmod{N} \\ 0 & j \neq 0 \pmod{N} \end{cases} \quad (3)$$

where the sum of the series is the total number of elements for $a_i = 1$ in a given period, T .

The detection signal, y_i , is given by the convolution of the modulation signal, x_i , and the atmospheric response function, G_i .

$$y_i = \sum_{j=0}^{N-1} x_{i-j} G_j + b + n_i \quad (4)$$

Where b and n_i are related to background and detector's noise, respectively. The modulated signal is repeatedly accumulated over M-time periods.

$$z_i = \sum_{k=1}^M y_{i+(k-1)N} \quad (5)$$

And by taking the cross-correlation S_i with the modulation code a'_i as,

$$S_i = \sum_{i=0}^{N-1} z_i a'_{i-1} \quad (6)$$

the response function G_i can be derived. This atmospheric response describes the spatial profile of the target.

From these equations, the SNR for the RMCW lidar can be represented with respect to the expectation value $E[S_i]$ and the standard deviation.

$$\left(\frac{S}{N}\right)_{RMCW} = \frac{\bar{S}_i}{\sqrt{V[S_i]}} = \frac{\sqrt{M}\xi P_o(N+1)G_i/2}{\sqrt{N}\sqrt{\xi\mu[P_o(N+1)]\bar{G}_i/2 + b}} \quad (7)$$

The excess noise factor of the detector μ is 2-3.

4. SNR Simulation

The LED mini lidar system parameters are enumerated in Table 1. The RM-CW LED lidar has the same system parameters except for the average output power (P_o : 38mW), pulse repetition frequency (continuous) and pulse width (8 ns or 12 ns). In order to have another point of comparison, we also simulated the SNR of a pulse modulated LD lidar. The LD lidar's system parameters are based from Takeuchi, et al. lidar system⁴) except for the output peak power (1 W) and the modulation type (pulse mode at 1 kHz). Two types of M sequence: PRBS-8 (255 bits) and PRBS-12 (4095 bits) with 1 code cycle period of 2 μ s and 49 μ s, respectively, were simulated. Choosing two different PRBS codes illustrates their effect on the SNR calculations. PRBS-8 ($\Delta t = 8$ ns) has a code length period of 2 μ s, which closely resembles the pulse repetition frequency (500 kHz) of the current pulse modulated LED lidar.

From the simulated SNR result on Fig. 3, we can observe an improvement of 4 orders of magnitude increase for the LED lidar if the RM-CW technique is used in the light transmission. Comparing with the simulated SNR of the pulse modulated LD lidar, the RM-CW LED lidar shows 2-3 orders of magnitude higher in daytime measurement.

Table 1. LED Lidar specifications

Transmitter		Receiver	
Light Source	NUV-LED NCSU034B (Nichia Corp.)	Cassegrain	
Wavelength	$\lambda = 385$ nm	Primary Mirror Aperture	10 cm ϕ
Beam Divergence	70 mrad	Primary Mirror Focal Length	72.25 mm
Beam Size	3 cm ϕ	Secondary Mirror Diameter	2.5 cm ϕ
Pulse		Secondary Mirror Focal Length	-25 mm
Pulse Width	10 ns	F.O.V.	3 mrad
Peak Power	$P_p = 0.75$ W	Aperture	1 mm
Pulse-Repetition Frequency	500 kHz	Sensor	PMT Hamamatsu R6350
Modulation			
Ave Power	$P_o = 37$ mW (PRBS-8) $P_o = 21$ mW (PRBS-12)	Number of elements	$N = 255$ (2^8-1) $N = 4095$ ($2^{12}-1$)
clock time	$\Delta t = 8$ ns (PRBS-8) $\Delta t = 12$ ns (PRBS-12)	Period	$T = 2$ μ s (PRBS-8) $T = 49$ μ s (PRBS-12)

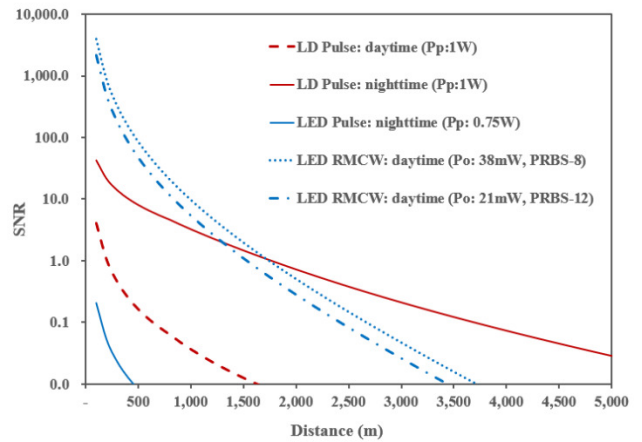


Fig. 3. Simulated SNR of a pulse modulated LED mini lidar and an LD lidar, and RM-CW LED mini lidar with respect to 1 second integration time.

5. Summary

The challenge of quantitatively investigating the Mar's dust devils phenomena arise for a construction of an LED mini lidar. It was field tested to observe different fast-moving targets in the near-range. Currently, it is limited to nighttime measurement. Thus, the need to increase its SNR is important. From the simulation result, the RM-CW technique was observed to increase the SNR of an LED mini lidar by 4 orders of magnitude.

The current photon counter has the capability to generate the RM-CW code. Moreover, linearity of the photon counter to an electrical RM-CW signal has already been verified. This ensures a complete overlap of each randomly arranged pulses per iteration count. The next step is to implement the RM-CW technique in actual LED lidar observation.

References

- 1) Shiina, T., Yamada, S., Senshu, H., Otobe, N., Hashimoto, G. L., and Kawabata, Y., 2016: LED mini lidar for Mars rover, *Proc. SPIE 10006*, 10006-15 pp.
- 2) Ong, P.M., Shiina, T., Kuze, H., et al., 2018, Compact LED lidar system fitted for a mars rover – design and ground experiment, *Proceedings of 28th International Laser Radar Conference*, EPJ Web of Conferences **176**, 02013 (2018).
- 3) Takeuchi, N., et al.: *Applied Optics* **22**, 9 (1983) 1382-1386.
- 4) Takeuchi, N., et al. *Applied Optics* **25**, 1 (1986) 63-67.
- 5) Ueno, T., Takeuchi, N. Baba, H., Sakurai, K., *The Review of Laser Engineering*, **16**, 3 (1988) 101-118.